WALOP's Spatial Distortion Modeling and CCD Photometry Pipeline

Shrish
Supervisors: Dr. Tuhin Ghosh and Prof. A.N. Ramaprakash

National Institute of Science Education and Research

27 November 2019

Outline

PASIPHAE Survey

PASIPHAE acronym for PASIPHAE acronym for **Polar-Areas Stellar Imaging Polarization High-Accuracy Experiment(Tassis et al. 2019)**.

PASIPHAE Objectives:

1. Measure optical polarisation of stars upto 0.3% in Galactic polar regions with 0.1% accuracy.
2. Cover about 4000 square degrees of of sky.
3. Measure polarisation of about 10^6 stars.
4. SNR ≥ 3 for stars $R \leq 16.5$.
5. Understanding interstellar dust clouds and magnetic field within it lies.

PASIPHAE

through the veil of dust to inflation

PASIPHAE Collaboration

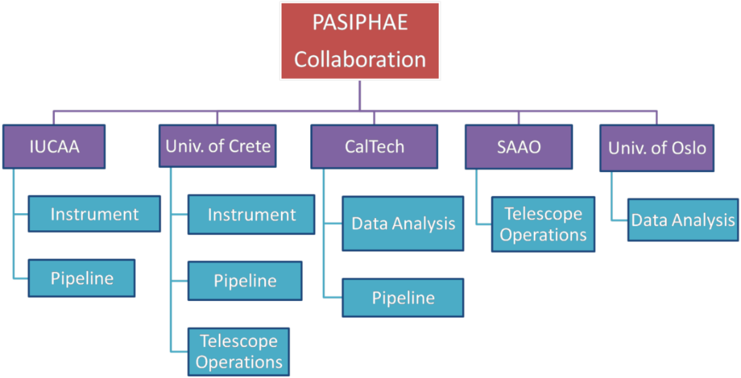

Science Goals

CMB B-mode Contamination

CMB B-mode(experiments searching for inflationary gravitational waves) signals are contaminated largely by polarised emission of cold dusts in CMB region(BICEP2/Keck Collaboration et al. 2015).

Dust Polarization Map

Dust polarization map is available for far-infrared region(350 GHz). But it is not always correlated with polarization map at CMB region(60-150 GHz). Because of temperature and magnetic field differences(Tassis Pavlidou 2015;Planck Collaboration et al. 2017, 2018).

3-D Magnetic Field Tomography

Knowledge of magnetic field in the dust cloud will help mapping dust polarization for CMB region and component separation of CMB B-mode signals.

Science Goals

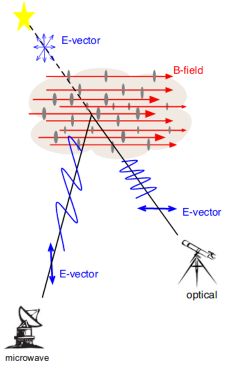

Figure: The same dust grain that radiates polarized emission in CMB region induces starlight polarization in optical region. Dust grains align their short axis with the direction of the magnetic field.

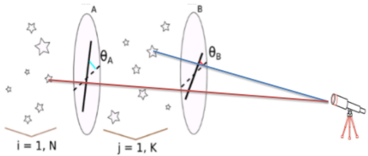

Figure: With distance information we can deduce direction of ISM magnetic field in sky plane in presence of dust clouds.

Stokes Parameters

A generalised formalism to observe all polarization states of radiations.

$$I = I_{0^\circ} + I_{90^\circ}$$
$$Q = I_{0^\circ} - I_{90^\circ}$$
$$U = I_{45^\circ} - I_{135^\circ}$$
$$V = I_{RCP} - I_{LCP}$$

$$p = \sqrt{q^2 + u^2}$$
$$\psi = \frac{1}{2}\tan^{-1}\frac{u}{q}$$
$$q = \frac{Q}{I}, u = \frac{U}{I}$$

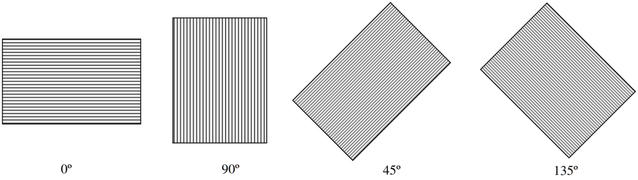

Figure: Measuring Stokes parameter with simple polarizer.

Wide Area Linear Optical Polarimeter(s)(WALOP)

- Measures q and u in one shot(Ramapraksh et al. 201$
- $q = \frac{N_0 - N_1}{N_0 + N_1}$
- $u = \frac{N_2 - N_3}{N_2 + N_3}$
- $\sigma_q = \sqrt{\frac{4\left(N_1^2\sigma_0^2 + N_0^2\sigma_1^2\right)}{(N_0+N_1)^4}}$
- $\sigma_u = \sqrt{\frac{4\left(N_3^2\sigma_2^2 + N_2^2\sigma_3^2\right)}{(N_2+N_3)^4}}$

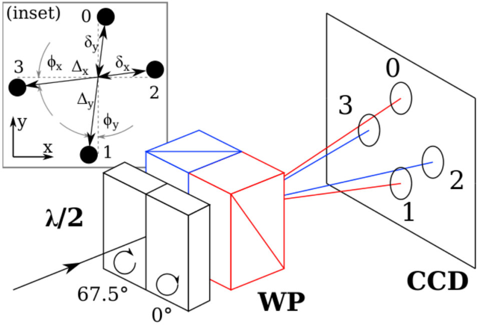

Figure: RoboPol concept: Four channel one-shot linear polarimetry.

4-beam Output of WALOP

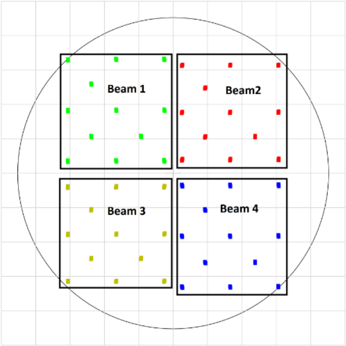

Figure: 4-beams on 4-CCDs

Distortion Map

- Modeled with 4-D general polynomials.
- $x = f_x(x', y')$
- $y = f_y(x', y')$
- $error = |\vec{r}_{\mathrm{data}} - \vec{r}_{\mathrm{model}}|$
- Used ensemble and cross matching techniques to create 4000 data points.
- Used Stochastic Gradient Descent Method(SGDM) to minimize the cost function.

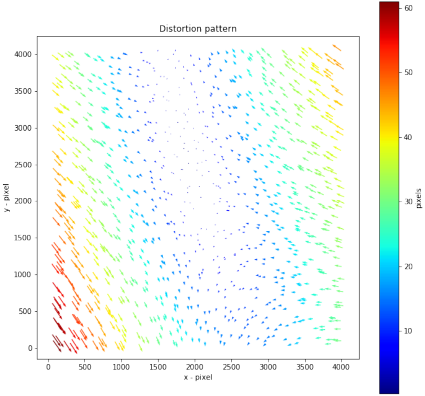

Figure: Spatial distortion map for WALOP output(beam-1).

Performance of the Model

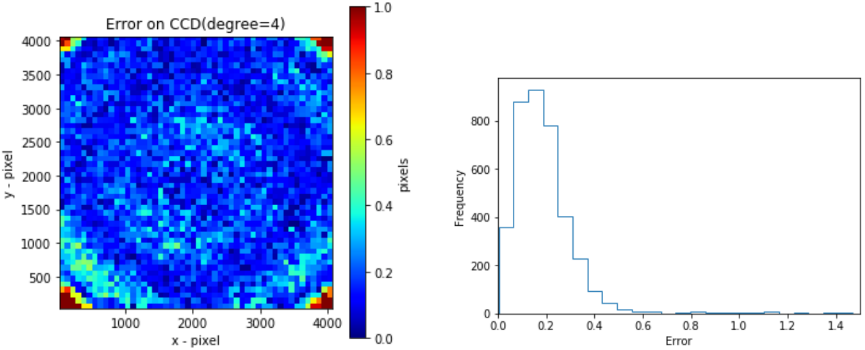

Figure: Left: Errors in predicting real coordinates. Right: Histogram of errors. Errors are less then 0.5 pixel except for corners.

Performance of the Model

Error Analysis (Total 3800 points)			
Degree(max) of general polynomial	Number of star points with error>0.25 pixel	Number of star points with error>0.5 pixel	Number of star points with error>1.0 pixel
2	1504(39.6%)	219(5.8%)	72(1.9%)
3	1566(41.2%)	152(4%)	44(1.2%)
4	830(21.1%)	75(1.2%)	29(0.76%)

- Error in estimating centroids of stars has maximum contribution on photometry error.
- We needed to cross match stars of different CCDs before performing relative photometry to get Stokes parameters.

Aperture Photometry

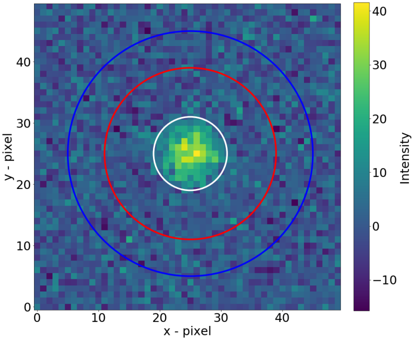

Figure: Aperture Photometry

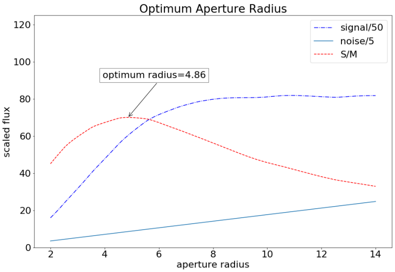

Figure: Growth curve analysis

Point Spread Functions(PSF) Modeling

- Given long distance in compare to size, stars are point source(angular spread less then dimension of a pixel of CCD).
- Point Spread Function(PSF) is the shape that a point source takes on CCD. Depends upon atmosphere(seeing) and all cumulative effects of the instruments.
- PSF modeling to perform high accuracy photometry.
  - Analytical Model(2-D functions)
  - Digital Model(Matrices)
- Analytical Model: 2-D orthogonal polynomials and elliptical Gaussian function.
- Iteratively Subtracted PSF Photometry technique.

PSF Photometry

- Aperture photometry fails badly in crowded field and contamination.
- Accuracy is limited by maximum S/N(growth curve).
- PSF photometry assigns a lower weight to lower S/N pixels and a higher to the higher S/N pixels.
- $Flux\ Total = \frac{\sum_i P_i \times PSF_i/\sigma_i^2}{\sum_i PSF_i^2/\sigma_i^2}$
- $\sigma_{\text{total}} = \frac{\sigma_{sky}}{\sqrt{\sum_i PSF_i}}$
- $\frac{\sigma(\text{aper})}{\sigma(psf)} = \sqrt{\sum PSF_i^2} * \sqrt{P} \geq 1$

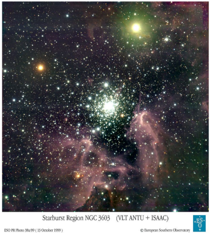

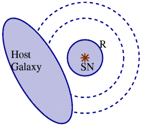

Figure: Crowded field and Contamination.

WALOP: The Worst Case PSFs

- Generally PSF is more or less same throughout the field.
- WALOP has PSF varying with field of view.
- We need to model PSF very accurately with respect to CCD coordinates.
- Existing photometry software is not up to the mark for WALOP.

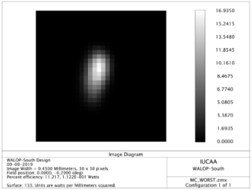

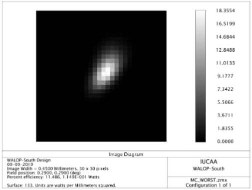

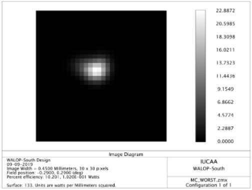

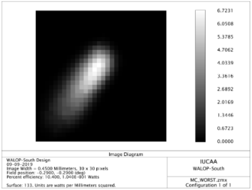

Photutils for WALOP Photometry

- Median error is 0.08%(quite good) for the best case.
- Median error is 1.2%(huge) for the worst case.
- Central area of CCD is performing better.
- We need photometry error to be less than 0.0001% for $p = 0.3\%$ and $\sigma_p = 0.1\%$.
- We need to customize the Python module according to our need.

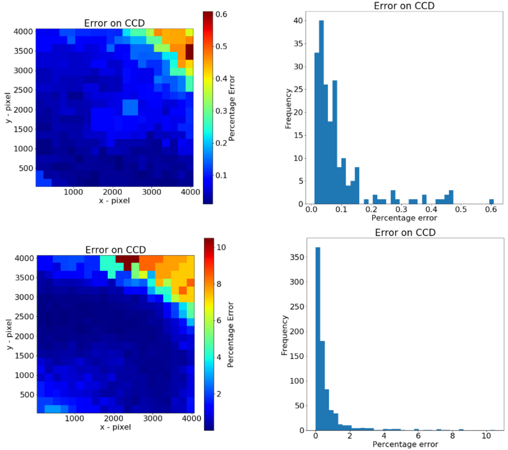

Figure: The best(up) and the worst(bottom) case.

Zernike Polynomials$(Z_n^m(\rho,\varphi))$

- $Z_n^m(\rho,\varphi) = R_n^m(\rho)\cos(m\varphi)$
  $Z_n^{-m}(\rho,\varphi) = R_n^m(\rho)\sin(m\varphi)$
- $R_n^m(\rho) = \sum_{k=0}^{\frac{n-m}{2}} \frac{(-1)^k(n-k)!}{k!\left(\frac{n+m}{2}-k\right)!\left(\frac{n-m}{2}-k\right)!}\rho^{n-2k}$
- $\rho = 1-\exp\left(\frac{-r}{\lambda}\right)$
- $PSF(r,\varphi) = \exp\left(-r^p\sum_{n,m} b_{n,m}Z_n^m(\rho,\varphi)\right)$
- Complicated model, hard to optimize.
- Highly unstable.
- Orthogonal only for unit disk.

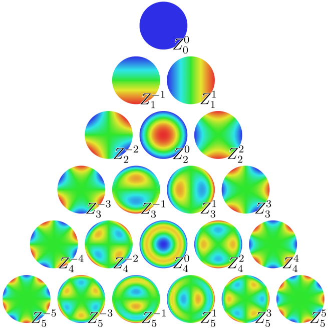

Figure: Some Zernike Polynomials.

Some Zernike PSFs

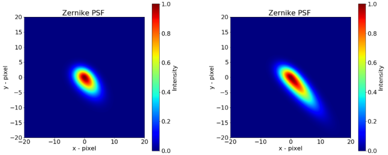

Figure: Left: $p = 2.0$, $b_{2,0} = 0.1$, $b_{1,-1} = 0.04$, and $b_{2,-2} = 0.04$. Right: $p = 2.0$, $b_{2,0} = 0.1$, $b_{1,-1} = 0.036$, and $b_{2,-2} = 0.065$.

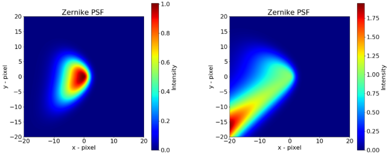

Figure: Left: $p = 2.0$, $b_{2,0} = 0.1$, $b_{1,-1} = 0.007$, $b_{1,1} = 0.12$ and $b_{4,2} = 0.04$. Right: $p = 2.0$, $b_{2,0} = 0.1$, $b_{1,-1} = 0.007$,$b_{1,1} = 0.13$ and $b_{4,2} = 0.04$. See how unstable the PSF is with respect to the parameter $b_{1,1}$.

Polar Shapelets$(\chi_{n,m}(r,\varphi;\beta))$

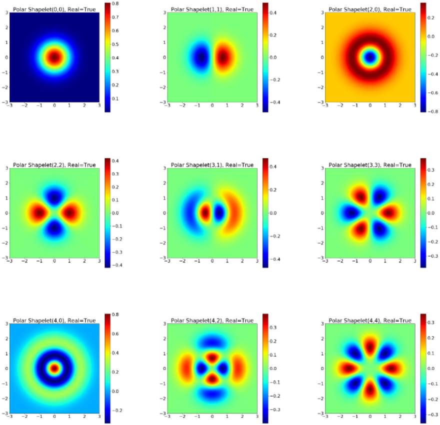

Figure: Real part of some polar shapelets.

Polar Shapelets

- $PSF(r,\varphi) = \sum_{n=0}^{n=\infty} \sum_{m=-n}^{m=n} b_{n,m}\chi_{n,m}(r,\varphi;\beta)$
- $b_{n,m} = \iint_R PSF(r,\varphi)\chi_{n,m}(r,\varphi;\beta)dr d\varphi$
- $\chi_{n,m}(r,\varphi;\beta) =$
$$\frac{(-1)^{\frac{n-|m|}{2}}}{\beta^{|m|+1}}\left[\frac{\left(\frac{n-|m|}{2}\right)!}{\pi\left(\frac{n+|m|}{2}\right)!}\right]^{\frac{1}{2}} \times r^{|m|} L^{|m|}_{\frac{n-|m|}{2}}\left(\frac{r^2}{\beta^2}\right)\exp\left(\frac{-r^2}{2\beta^2}\right)\exp(im\varphi)$$
- $L_x^k(x) = \frac{1}{x!}\sum_{i=0}^{i=x}\frac{x!}{i!}\left({}^{k+x}C_{n-i}\right)(-x)^i$
- This is not limited to unit disk and can be used directly as image components, unlike Zernike Polynomials.
- These are very intuitive in nature and widely used for morphological classification of images.
- Overlap integral can be solved using HealPy without having a optimizing problem.

Elliptical Gaussian Model

- $PSF(x,y) = I_o\left(1 + z^2 + \frac{1}{2}\beta_4 z^4 + \frac{1}{6}\beta_6 z^6\right)$
- $z^2 = \frac{1}{2}\left(\frac{x^2}{\sigma_x^2} + 2\sigma_{xy}xy + \frac{y^2}{\sigma_y^2}\right)$
- Simple to model and optimize.
- We don't need coordinate transformation.
- Most of the region(around the center) of CCD can be modeled alone with this. For the corner part, we will have to model residuals too(with Polar Shapelets).
- Parameters varies smoothly with CCD coordinates. We plan to divide CCD into some optimum part to perform further photometry.

Performance

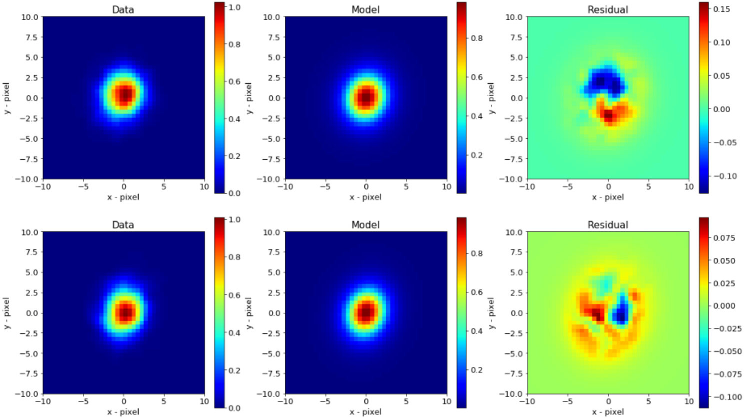

Figure: Fitting elliptical Gaussian with data. Some residuals have pattern and some are quite random. Up: $\sigma_x = 3.620$, $\sigma_y = 4.598$, $\sigma_{xy} = -0.038$, Bottom: $\sigma_x = 3.703$, $\sigma_y = 4.417$, $\sigma_{xy} = -0.0978$

Future Plans

- We plan to customize PSF modeling part of Photutils project according to our need.
- We shall try digital model instead of the analytical model.
- We may need to work on the centroid algorithm, which is used for finding stars on CCD image. Error in estimating centroid has largest contribution in photometry error.
- In wake of recent developments in machine learning algorithm. We may try some more efficient techniques to find the centroid and image processing.

References

[Ramapraksh et al. 2019] RoboPol: A four-channel optical imaging polarimeter
https://arxiv.org/abs/1902.08367

[Tassis et al. 2019] PASIPHAE: A high-Galactic-latitude, high-accuracy optopolarimetric survey
https://arxiv.org/pdf/1810.05652.pdf

[King et al. 2018] The RoboPol Pipeline and Control System
https://arxiv.org/pdf/1310.7555.pdf

[4] Why PSF fitting?
http://web.ipac.caltech.edu/staff/fmasci/home/astro_refs/WhyPSFfit.pdf

[Kenneth J. Mighell 1999] Algorithms of CCD photometry.
https://www.adass.org/adass/proceedings/adass98/mighellkj/

[Stetson et al. 1987] Daophot https://iopscience.iop.org/article/10.1086/131977

[Anderson et al. 2000] Building an EPSF.
https://iopscience.iop.org/article/10.1086/316632

[L. W. Piotrowski et al. 2013] Zernike polynomials. https://arxiv.org/abs/1302.0145

[Richard Massey et al. 2004] Polar Shapelets.
https://arxiv.org/abs/astro-ph/0408445

Thanks

Cosmic Dust

- Cosmic Dust, Dust, Extra Terrestrial Dust, Space dust are same thing.
- Size= Few molecules to 0.1 μm
- Asymmetric dust grains tends to orient their short axis with the magnetic field (Radiative Alignment Torque Theory). They emits polarised emission in far infra red region(350 GHz) and also in the CMB region(60-150 GHz)(cold dusts) but their polarization properties cannot be extrapolated to lower frequency. Reason of decorrelation can be different magnetic field and different temperature of the dust cloud.
- When star light passes through dust cloud they polarize parallel to the magnetic field.(Dichroic extinction effect)
- Polarized thermal dust emission from our Galaxy is major obstacle in the search for the primordial B-mode signal in the polarization of CMB.
- Earth is travelling through a dust veil of $10^{-6} dust/m^3$.

Cosmic Dust

- Thermal emission cannot provide this information because its intensity is the result of integration along the line-of-sight to infinity, and there fore distance information is lost. Stellar polarization, on the other hand, only traces the dust column out to the distance of the star.With enough measurements of stars of known distances tracing a similar sight line, one can reconstruct the plane-of-sky magnetic field orientation as a function of distance.

Signal To Noise

- If the number of photons received in a fixed interval of time has an average value N, but the photons are randomly spaced, the probability of detecting k photons in the fixed time interval is given by the Poisson distribution, $P(k) = \frac{N^k e^{-N}}{N!}$. For $N \geq 5$ $P(k) = \frac{1}{\sqrt{2\pi\sigma^2}} e^{-(k-N)^2/2\sigma^2}$ with $\sigma = \sqrt{N}$.